Upgrade of the Pierre Auger Observatory (AugerPrime)

C. Bleve [1,2], G. Cataldi[2], M. R. Coluccia[1,2], P. Creti[2] I. De Mitri[1,2], G. Fiore[2], G. Marsella[1,2], A. Miccoli[2], D. Martello[1,2], L.Perrone[1,2], C. Pinto[1,2] V. Scherini[1,2]

[1] Dipartimento di Matematica e Fisica "Ennio De Giorgi", Università del Salento, Italy
[2] Istituto Nazionale di Fisica Nucleare sez. di Lecce, Italy

1. Abstract

The data collected with the Pierre Auger Observatory have led to a number of surprising discoveries. While a strong suppression of the particle flux at the highest energies has been established unambiguously, the dominant physics processes related to this suppression could not be identified. Within the energy range covered by fluorescence detector observations with sufficient statistics, an unexpected change of the depth of maximum distribution is found. Using LHC-tuned interaction models these observations can be understood as a correlated change of the fluxes of different mass groups. On the other hand, they could also indicate a change of hadronic interactions above the energy of the ankle. Complementing the water Cherenkov detectors of the surface array with scintillator detectors will, mainly through the determination of the muonic shower component, extend the composition sensitivity of the Auger Observatory into the flux suppression region. The upgrade of the Auger Observatory will allow us to estimate the primary mass of the highest energy cosmic rays on a shower-by-shower basis. In addition to measuring the mass composition the upgrade will open the possibility to search for light primaries at the highest energies, to perform composition-selected anisotropy studies, and to search for new phenomena including unexpected changes of hadronic interactions. After introducing the physics motivation for upgrading the Auger Observatory the planned detector upgrade is presented. In the second part of the contribution the expected performance and improved physics sensitivity of the upgraded Auger Observatory are discussed.

2. Introduction

Measurements of the Auger Observatory [1] have dramatically advanced our understanding of ultra-high energy cosmic rays (UHECRs). Particularly exciting is the observed behavior of the depth of shower maximum with energy, which changes in an unexpected, non-trivial way. Around 3×10^{18} eV it shows a distinct change of slope with energy, and the shower-to-shower variance decreases [2]. Interpreted with the leading LHC-tuned shower models, this implies a gradual shift to a heavier composition [3]. A number of fundamentally different astrophysical model scenarios have been developed to describe this evolution, see, for example, [4, 5, 6, 7, 8]. The high degree of isotropy observed in numerous tests of the small-scale angular distribution of UHECRs above 4×10^{19} eV is remarkable [9], challenging original expectations that assumed only a few cosmic ray sources with a light composition at the highest energies. Interestingly, the largest departures from isotropy are observed for cosmic rays with $E > 5.8\times10^{19}$ eV in $\sim20^\circ$ sky windows [9, 10].

Due to a duty cycle of $\sim$15% of the fluorescence telescopes, the data on the depth of shower maximum extend only up to the flux suppression region, i.e., 4×10^{19} eV. Obtaining more information on the composition of cosmic rays at higher energies is of central importance for making further progress in understanding UHECRs. Care must be taken, since precision Auger measurements of shower properties, strongly constrained by the hybrid data, have revealed inconsistencies within present shower models, opening the possibility that the unexpected behavior is due to new hadronic interaction physics at energy scales beyond the reach of the LHC.

The aim of the upgrade of the Auger Observatory, collectively dubbed AugerPrime, is to provide additional measurements of composition-sensitive observables to allow us to address the following questions: (i) Elucidate the mass composition and the origin of the flux suppression at the highest energies, i.e., the differentiation between the energy loss effects due to propagation, and the maximum energy of particles injected by astrophysical sources. (ii) Search for a flux contribution of protons up to the highest energies. We aim to reach a sensitivity to a contribution

as small as 10% in the flux suppression region. The measurement of the fraction of protons is the decisive ingredient for estimating the physics potential of existing and future cosmic ray, neutrino, and gamma-ray detectors; thus prospects for proton astronomy with future detectors will be clarified. Moreover, the flux of secondary gamma rays and neutrinos due to proton energy loss processes will be predicted. (iii) Study extensive air showers and hadronic multiparticle production. This will include the exploration of fundamental particle physics at energies beyond those accessible at terrestrial accelerators, and the derivation of constraints on new physics phenomena, such as Lorentz invariance violation or extra dimensions.

The needed composition-sensitive information can be obtained by upgrading the Auger Observatory. In Sec. 3 a brief overview of the planned hardware upgrades is given, focusing on new scintillation detectors. The expected physics performance reached with the upgraded Observatory is illustrated in Sec. 4 using detailed simulations of different composition scenarios.

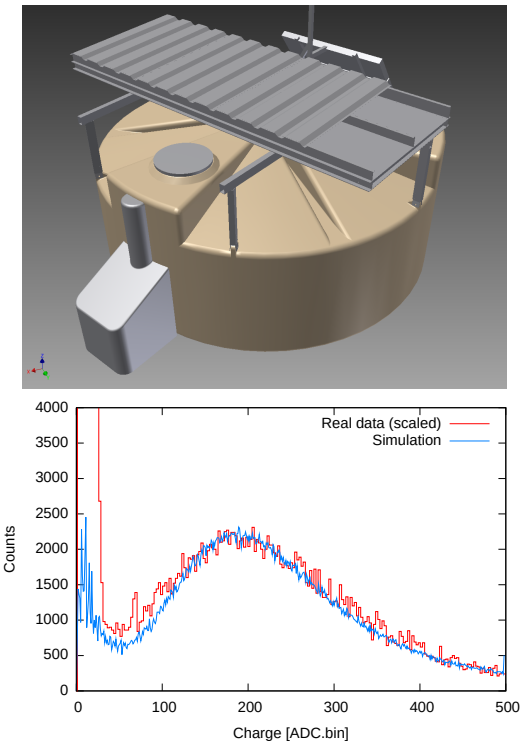

Figure 1. Top panel: 3D view of a SSD mounted on a WCD. A double roof, with the upper layer being corrugated aluminum (here shown partially cut away for clarity), is used to reduce the temperature variations. Bottom panel: MIP histogram taken with a $2\,\mathrm{m}^2$ prototype installed in the Auger array. The data correspond to one minute of data taking and are well reproduced by the detector simulation based on Geant 4.

3. Planned upgrade

The key element of the upgrade will be the installation of a new detector consisting of a plastic scintillator plane above each of the existing water-Cherenkov detectors (WCD). This scintillation detector will provide a complementary measurement of the shower particles: they will be sampled with two detectors having different responses to muons and electromagnetic particles, allowing the reconstruction of the different components. The design of the surface scintillator detectors (SSD) is simple, reliable and they can be easily deployed over the full $3000\,\mathrm{km}^2$ area of the overall Auger Surface Detector (SD). An SSD unit will consist of a box of $3.8\,\mathrm{m} \times 1.3\,\mathrm{m}$, housing two scintillator modules, each covering an area of $1.9\,\mathrm{m}^2$, see Fig. 1 (top). The 1 cm thick scintillators are read out by wavelength-shifting fibers guiding the light of the two modules to a PMT. The deviations from a uniform detector response over the area of the scintillator are smaller than 5%. The SSD is triggered by the larger WCD, resulting in a clean separation of the MIP signal from the background, see Fig. 1 (bottom). An engineering array of 10 detectors will be installed at the Auger site in 2016.

The SD stations will be upgraded with new electronics that will process both WCD and SSD signals. Use of the new electronics also aims to increase the data quality (with faster sampling of ADC traces, better timing accuracy, increased dynamic range), to enhance the local trigger and processing capabilities (with a more powerful local station processor and FPGA) and to improve calibration and monitoring capabilities of the surface detector stations. The signals of the WCDs and SSDs will be sampled synchronously at a rate of 120 MHz (previously 40 MHz) and the GPS timing accuracy will be better than 5 ns. The dynamic range of the WCDs will be enhanced by a factor of 32 due to the new electronics and an additional small 1″ PMT that will be inserted in one of the filling ports. First prototypes of the new electronics have been built and are being tested. Both the SSDs and the electronics upgrade can be easily deployed, and will have only minimal impact on the continuous data taking of the Observatory.

A network of underground muon detectors, part of the AMIGA [1, 11] system, is now being deployed in the existing SD infill area of $23.5\,\mathrm{km}^2$.

This will provide important direct measurements of the shower muon content and its time structure, while serving as verification and fine-tuning of the methods used to extract muon information with the SSD and WCD measurements.

In parallel with the SD upgrade, the operation mode of the Fluorescence Detector (FD) [12] will be changed to extend measurements into periods with higher night sky background. This will allow an increase of about 50% in the current duty cycle of the FD.

4. Expected physics performance

In the following we consider different levels of complexity of the information derived from shower data. We first discuss the reconstruction of the muonic shower component, then show the discrimination power for different primary particles, and finally analyze Monte Carlo generated event samples to test the sensitivity to different physics scenarios. As a generic measure of discrimination power for separating primary i and j using the corresponding observables S_i and S_j (with the RMS σ) we use the merit factor

$$f_{\mathrm{MF}} = \frac{|\langle S_i\rangle - \langle S_j\rangle|}{\sqrt{\sigma(S_i)^2 + \sigma(S_j)^2}}. \qquad (1)$$

4.1. Event based observables

The least model-dependent and most direct composition-sensitive observable that can be obtained from the upgraded detector array is the number of muons (or, equivalent to it, the muonic signal in the WCD) in individual detector stations. Thanks to the signal responses in the SSD (S_{SSD}) and the WCD (S_{WCD}) to particles of the electromagnetic and muonic shower components, it is possible to derive the muonic signal $S_{\mu,\mathrm{WCD}}$ on a station-by-station basis, as described in [13], from

$$S_{\mu,\mathrm{WCD}} = a\, S_{\mathrm{WCD}} \;+\; b\, S_{\mathrm{SSD}}, \qquad (2)$$

where the signals are measured in units of the response to a vertical equivalent muon (VEM) or minimum ionizing particle (MIP), respectively. The factors a and b are derived from detector simulation and have only a very weak dependence on the primary composition and lateral distance from the shower core. Restricted by the limited size of an individual detector station, this method is subject to large fluctuations and is only well suited for deriving mean muon numbers, see Fig. 2 (top).

The performance of the reconstruction of the muonic signal is considerably improved by fitting a lateral distribution function (LDF) to the signals. Eq. 2 is then applied to the LDF values for

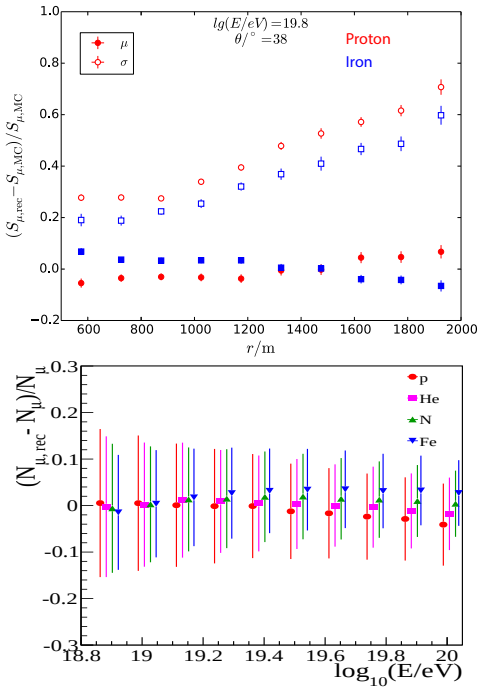

Figure 2. Top panel: Reconstruction bias (solid symbols) and resolution (open symbols) of the muonic signal contribution for individual detector stations, as a function of distance r from the shower core. The results for proton and iron showers are shown in red and blue, respectively. Bottom panel: Number of muons N_μ reconstructed for individual showers using shower universality, compared with the true N_μ as a function of energy for different primary species. Error bars represent the RMS of the distributions.

the WCD and SSD to calculate the muonic signal at an 800 m core distance, $S_\mu(800)$. Reconstruction resolutions of the muonic signal of, for example, $\sigma[S_\mu(800)]/\langle S_\mu(800)\rangle \approx 22\%$ for protons and $\sigma[S_\mu(800)]/\langle S_\mu(800)\rangle \approx 14\%$ for iron are reached at $E \approx 10^{19.8}$ eV and $\theta = 38°$. Using $S_\mu(800)$ as a composition estimator, the obtained merit factors for distinguishing between proton and iron primaries are above 1.5 at high shower energies ($E > 10^{19.5}$ eV) and small zenith angles.

An analysis based on shower universality (see [14] and references therein), or a sophisticated multivariate analysis, allows one to correlate the detector signals at different lateral distances and also takes advantage of the arrival time (shower front curvature) and temporal structure of the signal measured in the detectors. We are working on developing a reconstruction using all these observables. Some first results are given in the

following, but it should be kept in mind that the corresponding merit factors should be considered as lower limits to what will be reached after having a better understanding of the detectors. The universality-based reconstruction provides, in addition to the shower energy, the depth of shower maximum (mainly from the curvature of the shower front and the steepness of the lateral distribution) and the number of muons relative to the prediction of a reference model. The bias of the $X_{\rm max}$ reconstruction is below $15\,{\rm g/cm^2}$ with a resolution improving from $40\,{\rm g/cm^2}$ at $10^{19}\,{\rm eV}$ to $25\,{\rm g/cm^2}$ at $10^{20}\,{\rm eV}$. The corresponding results for the muon number reconstruction are shown in Fig. 2 (bottom). Of interest is also the energy resolution for the reconstruction which is about 10% at $10^{19}\,{\rm eV}$ down to 7% at $10^{20}\,{\rm eV}$. Examples of merit factors obtained by combining the two observables are 1.54 (proton-iron), 0.41 (proton-helium), and 0.64 (nitrogen-iron), all calculated for $10^{19.6}\,{\rm eV}$, zenith angles $\theta < 60^\circ$ and using QGSJet II.04.

4.2. Application to physics goals

Without knowing what composition to expect in the GZK suppression region it is difficult to demonstrate the potential of AugerPrime. Therefore, we have chosen two physics motivated benchmark models [15] fitted to the Auger flux [16] and composition data [3] for $E > 10^{18.7}\,{\rm eV}$, see Fig. 3, to illustrate the discrimination power of the additional information. Mock data sets were generated for these scenarios with a statistics corresponding to 7 years of data taking with AugerPrime. Only SD data are used in the reconstruction.

The mean $X_{\rm max}$, $\sigma(X_{\rm max})$, and the relative muon number R_μ are shown in Fig. 4. The $\sigma(X_{\rm max})$ contains the intrinsic air-shower fluctuations and the reconstruction resolution. While the mean $X_{\rm max}$, $\sigma(X_{\rm max})$ and R_μ are very similar up to $10^{19.2}\,{\rm eV}$, the energy range that is well covered by data of the fluorescence telescopes [2], the models predict significantly different extrapolations into the GZK suppression region. This difference is well reproduced with the reconstructed $X_{\rm max}$, $\sigma(X_{\rm max})$ and R_μ and the two scenarios can be distinguished with high significance and statistics.

As a next step we want to illustrate the increased sensitivity of AugerPrime with a more specific example. We use the arrival directions of the 454 measured events with $\theta < 60^\circ$ and energy higher than $4{\times}10^{19}\,{\rm eV}$ (see [9]) and randomly assign each event an $X_{\rm max}$ value according to model 1 (maximum-rigidity scenario). To implement a 10% proton contribution we assigned

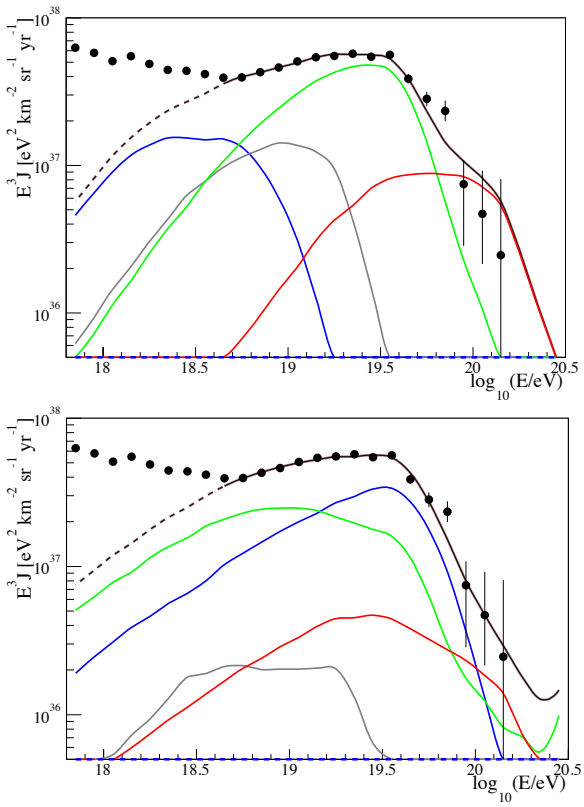

Figure 3. Benchmark spectra chosen as representations of a maximum-rigidity scenario [4] (top panel) and one photo-disintegration scenario (bottom panel). The index of the injection energy spectrum at the sources is about -1 (-2) for the maximum-rigidity (photo-disintegration) scenario – for details see [15]. The colors for the different mass groups are protons – blue, helium – gray, nitrogen – green, and iron – red.

10% of the events a proton-like $X_{\rm max}$. Half of these randomly chosen, proton-like events were given arrival directions that correlate with AGNs with a distance of less than 100 Mpc of the Swift-BAT catalog [17] within 3°. The other half were chosen with larger angular distances. By construction, this artificial data set reproduces many arrival direction features found in the Auger data while at the same time having a model-predicted mass composition.

Analyzing this data set without using any composition information, a correlation with the AGNs of the Swift-BAT catalog is found at a level similar to that reported in [9]. The improvement of the sensitivity in finding the correlation with AGNs in this data set is shown in Fig. 5 for $E > 4{\times}10^{19}\,{\rm eV}$. The top panel gives the result of the complete data set and the bot-

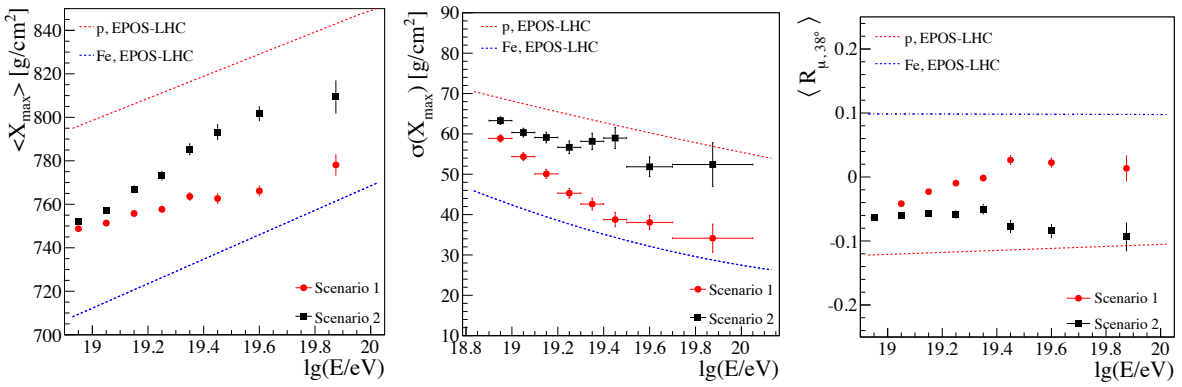

Figure 4. Reconstructed mean depth of shower maximum $X_{\rm max}$ (left) and its fluctuations (center), and the mean number of muons at 38° (right) using only SD data. Shown are the two scenarios: (1) maximum-rigidity model; (2) photo-disintegration model. The $\sigma(X_{\rm max})$ contains the intrinsic air-shower fluctuations and the detector resolution. The number of muons is given relative to that expected for an equal mix of p-He-CNO-Fe as primary particles.

tom panel that of a proton-enriched sample. The proton-enriched sample is obtained by selecting events with a reconstructed $X_{\rm max}$ greater than $770\,{\rm g/cm^2}$ at $10^{19}\,{\rm eV}$, adjusted to the event energies with an elongation rate of $55\,{\rm g/cm^2}$ per decade. While the correlation of the arrival directions with that of AGNs in the Swift-BAT catalog is not significant for the complete data set, a correlation well in excess of 3σ can be found for the proton-enriched samples.

In addition to these studies, the availability of muon information on an event-by-event basis allows for many ways of studying features of hadronic interactions. For example, the correlation between the number of muons and the depth of shower maximum can be used to study general features of muon production, including the search for exotic interaction scenarios at very high energy [18].

5. Conclusions

The Auger upgrade promises high-quality future data, and real scope for new physics uses of existing events. With operation planned from 2018 until 2024, event statistics will more than double compared with the existing Auger data set, with the critical added advantage that every event will now have mass information. This will allow us to address some of the most pressing questions in UHECR physics, including that of the origin of the flux suppression, the prospects of light particle astronomy and secondary particle fluxes, and the possibility of new particle physics at extreme energies.

Obtaining additional composition-sensitive information will not only help to better reconstruct the properties of the primary particles at the highest energies, but also improve the measurements in the important energy range just above the ankle. Furthermore, measurements with the new detectors will help to reduce systematic uncertainties related to modeling hadronic showers and to limitations of reconstruction algorithms. This improved knowledge of air-shower physics will likely then also allow a re-analysis of existing data – for improved energy assignments, for mass composition studies, and for photon and neutrino searches.

Finally it should be mentioned that the addition of scintillator detectors across the entire Observatory will also make possible direct comparisons of Auger measurements with those of the surface detectors of the Telescope Array experiment. This will strengthen the already productive cooperation between the two Collaborations, which has an aim of understanding the highest energy cosmic ray flux across the entire sky.

REFERENCES

1. **Pierre Auger** Collaboration, A. Aab et al., *The Pierre Auger Cosmic Ray Observatory, to appear in Nucl. Instrum. Meth.* **A** (2015) [1502.01323].
2. **Pierre Auger** Collaboration, A. Aab et al., *Depth of maximum of air-shower profiles at the Pierre Auger Observatory. I. Measurements at energies above* $10^{17.8}$ *eV, Phys. Rev.* **D90** (2014) 122005, [1409.4809].
3. **Pierre Auger** Collaboration, A. Aab et al., *Depth of maximum of air-shower profiles at*

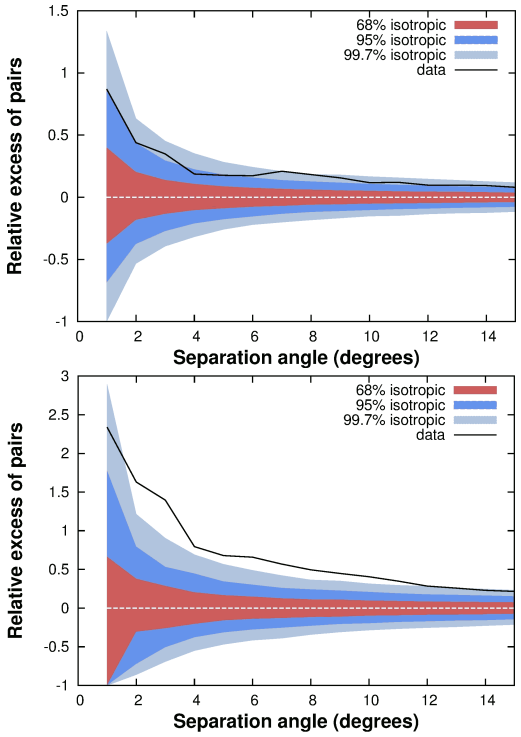

Figure 5. Angular correlation of cosmic rays of the modified Auger data set with AGNs of the Swift-BAT catalog [17]. Shown are distributions of relative excesses of pairs of events as a function of angular separation between them, for the complete data set (454 events, top) and the proton-enriched selection (128 events, bottom).

the Pierre Auger Observatory. II. Composition implications, *Phys. Rev.* **D90** (2014) 122006, [1409.5083].

4. D. Allard, *Extragalactic propagation of ultrahigh energy cosmic-rays*, *Astropart. Phys.* **39-40** (2012) 33–43, [1111.3290].
5. A. M. Taylor, *UHECR Composition Models*, *Astropart. Phys.* **54** (2014) 48–53, [1401.0199].
6. R. Aloisio, V. Berezinsky, and P. Blasi, *Ultra high energy cosmic rays: implications of Auger data for source spectra and chemical composition*, *JCAP* **1410** (2014) 020, [1312.7459].
7. N. Globus, D. Allard, and E. Parizot, *A complete model of the CR spectrum and composition across the Galactic to Extragalactic transition*, 1505.01377.
8. M. Unger, G. R. Farrar, and L. A. Anchordoqui, *Origin of the ankle in the ultra-high energy cosmic ray spectrum and of the extragalactic protons below it*, 1505.02153.
9. **Pierre Auger** Collaboration, A. Aab et al., *Searches for Anisotropies in the Arrival Directions of the Highest Energy Cosmic Rays Detected by the Pierre Auger Observatory*, *Astrophys. J.* **804** (2015) 15, [1411.6111].
10. **Telescope Array** Collaboration, R. Abbasi et al., *Indications of Intermediate-Scale Anisotropy of Cosmic Rays with Energy Greater Than 57 EeV in the Northern Sky Measured with the Surface Detector of the Telescope Array Experiment*, *Astrophys. J.* **790** (2014) L21, [1404.5890].
11. **Pierre Auger** Collaboration, B. Wundheiler et al., *The AMIGA Muon Counters of the Pierre Auger Observatory: Performance and Studies of the Lateral Distribution Function*, *Proc. of 34th Int. Cosmic Ray Conf., The Hague, PoS(ICRC2015)324* (2015).
12. **Pierre Auger** Collaboration, J. Abraham et al., *The Fluorescence Detector of the Pierre Auger Observatory*, *Nucl. Instrum. Meth.* **A620** (2010) 227–251, [0907.4282].
13. A. Letessier-Selvon, P. Billoir, M. Blanco, I. C. Mariş, and M. Settimo, *Layered water Cherenkov detector for the study of ultra high energy cosmic rays*, *Nucl. Instrum. Meth.* **A767** (2014) 41–49, [1405.5699].
14. M. Ave, R. Engel, J. Gonzalez, D. Heck, T. Pierog, and M. Roth, *Extensive air shower universality of ground particle distributions*, *Proc. of 31st Int. Cosmic Ray Conf., Beijing* **2** (2011) 178–181.
15. **Pierre Auger** Collaboration, A. di Matteo et al., *Combined fit of spectrum and composition data as measured by the Pierre Auger Observatory*, *Proc. of 34th Int. Cosmic Ray Conf., The Hague, PoS(ICRC2015)249* (2015).
16. **Pierre Auger** Collaboration, A. Aab et al., *The Pierre Auger Observatory: Contributions to the 33rd International Cosmic Ray Conference (ICRC 2013)*, *Proc of 33rd Int. Cosmic Ray Conf., Rio de Janeiro* (2013) [1307.5059].
17. W. Baumgartner, J. Tueller, C. Markwardt, G. Skinner, S. Barthelmy, et al., *The 70 Month Swift-BAT All-Sky Hard X-Ray Survey*, *Astrophys. J. Suppl.* **207** (2013) 19, [1212.3336].
18. J. Allen and G. Farrar, *Testing models of new physics with UHE air shower observations*, *Proc of 33rd Int. Cosmic Ray Conf., Rio de Janeiro* (2013) [1307.7131].